Irreversible frustrated spinodal decomposition in simultaneous interpenetrating polymer networks: Small-angle x-ray scattering

I. Alig and M. Junker
Deutsches Kunststoff-Institut, Schlossgartenstrasse 6, D-64289 Darmstadt, Germany

M. Schulz and H. L. Frisch
State University of New York at Albany, Department of Chemistry, Albany, New York 12222
(Received 7 November 1995)

A structure factor is derived in the hydrodynamic limit which reflects the development of a microphase structure during the formation of simultaneously cross-linked interpenetrating polymer networks (IPN's). This structure formation is a competitive process of spinodal decomposition and frustration of the fluctuations by increasing topological restraints due to network growth. The structure factor is compared with the scattering intensities from small-angle x-ray scattering performed on simultaneously cross-linked IPN's of poly(carbonate-urethane) and poly(methyl methacrylate). Experimental data and theory are in good agreement for all compositions. The results give an averaged characteristic length of the frozen fluctuations which is about 2 nm for samples having one thermodynamic glass transition, as determined by differential scanning calorimetry, and between 15 and 35 nm for samples having two glass transitions. In contrast to the structure factor for the microphase separation transition in homogeneous (ideal) IPN's or block copolymers which shows a q^2 and q^{-2} dependence at small and large scattering vectors q, respectively, the structure factor reveals a finite contribution in the limit $q \to 0$ and a q^{-4} behavior at large q values. A comparison of the data with the Debye-Bueche law yields also a good approximation at intermediate q values and indicates agreement with a more general treatment of scattering by an inhomogeneous solid.

I. INTRODUCTION

Interpenetrating polymer networks (IPN's) belong to the class of multiple-component polymer materials, which include polymer blends, block copolymers, and grafted networks. Each of these materials is based on a combination of two or more polymers. Since most of the polymers are immiscible, as a consequence of the small contribution from the mixing entropy of macromolecules to the free energy of mixing, phase separation takes place, leading to multiple phase morphologies in these materials. A study of the dynamics allows the determination of the time behavior of the phase separation, which depends on microscopic or mesoscopic parameters (e.g., self-diffusion and interdiffusion coefficients, binary thermodynamic interaction parameters, and process rates of possible underlying chemical reactions). In general two types of phase separation are distinguished: spinodal decomposition (SD) and nucleation and growth. Whereas the latter remains effective for the large time regime of the phase separation, the initial regime is mainly determined by SD. A mean field description of SD in metallic alloys was given by Cahn and Hilliard[1] and subsequently adapted to the case of polymer blends by de Gennes[2] and Binder.[3] The phase separation of blends and the resulting morphologies have been studied by means of time-resolved and static light and small-angle x-ray scattering,[4–6] revealing dispersed and cocontinuous structures with phase sizes of 10^2–10^4 nm. In the case of copolymers the tendency to phase separate is restricted due to chemical links between the different components and decomposition on a macroscopic scale is not possible. For block copolymers a microphase separation transition (MST) does occur, leading to regular lattice morphologies with microphase sizes of 10^2–10^3 nm. The MST and the structures in the phase-separated regime have been thoroughly investigated by transmission electron microscopy (TEM), small-angle x-ray scattering (SAXS) and small-angle neutron scattering (SANS) experiments, as well as by relaxation methods.[7,8] The theory of the MST for copolymers has been developed in the last decade based on a mean field approach taken by Leibler,[9] using the random phase approximation (RPA). The MST is controlled by two parameters, the product of the Flory interaction parameter and the chain length χN and the composition f. A MST has also been predicted by de Gennes[10] for a grafted network, which is formed by cross-linking two weakly incompatible linear polymers in their coexistence region and then cooled down below a transition temperature T_c, described in terms of the Flory interaction parameter χ and the average number of monomers between cross-links. An experimental confirmation has been done recently.[11]

IPN's are composed of two (or more) chemically distinct cross-linked networks of which at least one is synthesized in the presence of the other, which are held together predominantly by their trapped mutual entanglements rather than covalent bond grafting.[12,13] In the last two decades a wide variety of IPN's has been synthesized (sequential, simultaneous, latex, gradient, thermoplastic, semi) and their physical properties and structure have been studied by several methods including differential scanning calorimetry (DSC), TEM, dynamic mechanical analysis (DMA) , SAXS, and SANS,[14–18] Those investigations show that usually IPN's do not interpenetrate on a monomer scale, but have a microheterogeneous morphology with small regions enriched by segments of one of the components. This multiphase

structure results from the phase separation due to thermodynamic immiscibility of the networks, which arises during its formation at a definite degree of conversion in the course of the chemical reactions of polymerization and cross-linking. This effect should not be confused with a MST (Refs. 19–21) predicted for completed IPN's, which is due to the coexistence of repulsive potentials between both components and the microscopical deformation of the mutually entangled network chains, which leads to an attractive elastic force between both components. This effect is based on a homogeneous (disordered) phase, which undergoes a MST to an ordered phase of regular lattice morphology controlled by composition f and the Flory interaction parameter χ. Therefore the formation of such IPN's must occur without any phase decomposition. But, in general, nucleation and growth[22] and spinodal decomposition occur during the synthesis of both subnetworks, in which SD often predominates.[23]

In this paper a structure factor is derived in the hydrodynamic limit, which reflects the development of microphases due to spinodal decomposition during the formation of the network. This theory is compared with SAXS investigations of the morphologies of simultaneous IPN's of poly(carbonate-urethane) (PCU) and poly(methyl methacrylate) (PMMA), in which the monomers, cross-linkers, initiators, and catalysts for both networks are mixed in the initial state and the subsequent reactions leading to network formation occur simultaneously without any mutually interfering graft reactions. The analysis of the scattering data gives an estimation for the averaged characteristic length l of the frozen microphases. For comparison the data are also analyzed using the Debye-Bueche law.

II. EXPERIMENTAL DETAILS

A. Samples

The samples were synthesized under similar conditions as described in Ref. 24. The PCU network was prepared by cross-linking poly(1,6-hexane diol-carbonate) (PC) with the biuret triisocyanate (BTI) derived from hexamethylene diisocyanate via an addition reaction. The PMMA network was synthesized simultaneously by a free radical reaction using ethylene glycol dimethacrylate (EGDMA) as a cross-linker and a mixture of benzoyl peroxide (BPO)/*N*,*N*-dimethyl aniline (DMA) as an initiator redox system. From the molecular weights of the PC, M_w(PC)=850 (1100) g/mol, and the cross-linker used, M_w(BTI)=500 g/mol, the molecular weight between the cross-links M_c of the PCU network should be about 1180 (1430) g/mol. The typical M_c of cross-linked PMMA is about 4000 g/mol as calculated from the employed stoichiometry and determined by swelling measurements. The glass transition temperature T_g of all samples has been determined by DSC (Perkin Elmer, DSC 7). The measurements were carried out under a nitrogen atmosphere from -70 to 200 °C at a scanning rate of 20 °C/min for heating and cooling. The DSC data for the second heating are shown in Fig. 1 and the values for T_g are given in Table I. Two T_g's are found for the samples with 30 and 54 wt. % PCU (the second transition for sample 2 at T_g=127 °C is about 20 °C above the expected value for the PMMA component), whereas samples with higher PCU content, 60 and 80 wt. % have one T_g. This is in accordance with investigations on ageing in simultaneous IPN's of PCU/PMMA,[25] which show one T_g for all compositions measured by DSC immediately after their preparation and two T_g's for samples with lower PCU weight fraction measured 1.5 yr after their synthesis.

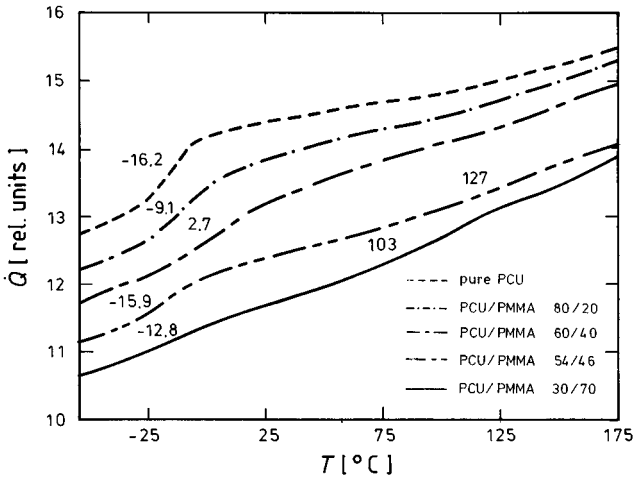

FIG. 1. DSC curves, relative heat flow versus temperature of IPN's, and cross-linked PCU.

B. SAXS Measurements

The SAXS measurements were performed with a Kratky Compact camera (A.Paar KG) equipped with a one-dimensional position-sensitive detector (M. Braun). Ni-filtered Cu $K\alpha$ radiation (λ=0.154 nm) was used. The sample was kept in the camera under vacuum to minimize air scattering. All data were taken at room temperature (T=20 °C). They were corrected for absorption, background scattering, slit length smearing,[26] and thermal fluctuations. Primary beam intensities were determined in absolute units (e.u.^{2}/nm^3) by using a moving-slit method.

III. SD IN SIMULTANEOUS IPN'S

A. Structure factor

For the data analysis a structure factor is derived, which reflects the frozen composition fluctuations due to spinodal decomposition during the formation of an IPN. We restrict ourselves in the following discussion to two-component IPN's, in which each component (A and B, respectively) forms a separate network. Both subnetworks are connected

TABLE I. Glass transition temperatures T_g of IPN's and cross-linked PCU, monomer unit volumes V_z of PCU, and electron density differences $\Delta\eta^2$ of IPN's.

Sample	PCU [wt. %]	$\overline{M_c}$ [PCU]	T_g [°C]	V_z [nm^3]	$\Delta\eta^2$ [e.u.^{2}/nm^6]
1	30	1180	−12.8, 103	0.83	139
2	54	1430	−15.9, 127	0.99	217
3	60	1180	2.7	0.83	172
4	80	1180	−9.1	0.83	317
5	100	1180	−16.2		

only by mutual entanglements. Usually, the simultaneous formation of IPN's starts from the monomers, which form during the IPN synthesis monotonously growing clusters (with a given time-dependent distribution). However, we can approximate the evolution of the IPN on a (preaveraged) mean field level by effective hydrodynamic equations with time-dependent coefficients. For each component the mass balance law holds in the hydrodynamic limit,

$$\frac{\partial \rho_i}{\partial t} + \mathrm{div}\, j_i = 0 \tag{1}$$

($i=A,B$). The current j_i can be described in a linear theory by $j_i = -\Lambda_{ik}\nabla\mu_k$, with the chemical potential μ_k and the generalized (nonlocal) Onsager coefficient Λ_{ik}. After introducing the order parameter $\psi(\mathbf{r})=(1-f)\rho_A(\mathbf{r})-f\rho_B(\mathbf{r})$ ($f=\langle\rho_A\rangle$, $1-f=\langle\rho_B\rangle$; f is the composition ratio), where $\rho_A(\mathbf{r})$ and $\rho_B(\mathbf{r})$ are the local concentrations of the two components at the point **r,** and an effective current $j=(1-f)j_A-f\ j_B$ and $\mu=(1-f)\ \mu_A-f\ \mu_B$, respectively, Fourier transformation of Eq. (1) yields

$$\frac{\partial}{\partial t}\psi(q) = -q^2\Lambda(q)\mu(q) + \eta(q,t), \tag{2}$$

where η is added to the linear response term to represent thermodynamic noise corresponding to inner degrees of freedom. The free energy density F for a polymer mixture in terms of the order parameter ψ is given by[27,28]

$$F = \frac{1}{N_a}\psi\ \ln\psi + \frac{1}{N_b}(1-\psi)\ln(1-\psi) - \chi\psi(1-\psi) + \frac{A}{2}|\nabla\psi|^2, \tag{3}$$

with the Flory-Huggins interaction parameter χ and $\sqrt{A}$ being the characteristic minimal length of the model (in the present case $\sqrt{A}$ is of the order of magnitude of the segment length). The effective chemical potential μ is the first derivative of F with respect to ψ. In a linear approximation of the Fourier transform we get

$$\mu = \frac{\partial F}{\partial\psi(q)} \simeq [Aq^2+m]\psi(q), \tag{4}$$

where m is the inverse structure factor $\lim_{q\to 0}S^{-1}(q)$ which is proportional to $T-T_c$ and A is proportional to the gradient energy coefficient. In the case of a distribution of molecules (cluster) of the two network components, A and m are effective values averaged over all molecules (we use the preaverage approximation). In the course of the chemical polymerization and cross-linking reactions during network formation, the mass and shape of the molecules and network fragments change. This suggests that an additional term is present in Eq. (4) which describes the topological connections of the growing network. Therefore in the simplest approximation A, m, and C become time dependent, $A\to A(t)$, $m\to m(t)$, $C\to C(t)$, and describe the chemical evolution of the system. For IPN's the free energy is given by[10,29,30]

$$F = \int\left[Aq^2+m+\frac{C}{q^2}\right]\psi(q)^2 d^3q, \tag{5}$$

$$\mu(q) = \left[A(t)q^2+m(t)+\frac{C(t)}{q^2}\right]\psi(t) = L(q,t)\psi(t), \tag{6}$$

where $C(t)$ represents the local attractive interaction that becomes effective when the first closed network loops are formed and elastic forces start to counteract the repulsion of the two network components. The chemical potential μ can now be substituted into Eq. (2) which yields

$$\frac{\partial}{\partial t}\psi(q) = -q^2\Lambda(q)L(q,t)\psi(q) + \eta(q,t). \tag{7}$$

The reciprocal Onsager coefficient can be represented by[3]

$$\frac{1}{\Lambda(q)} = \frac{1}{D_A S_A(q) f} + \frac{1}{D_B S_B(q)(1-f)}. \tag{8}$$

In the hydrodynamic limit the monomer structure factors $S(q)_i$, $i=A,B$, can be substituted by $S(0)_i$, which is equivalent to the averaged (and therefore also time-dependent) number of monomers per molecule, N_i. By assuming Rouse dynamics,[31] i.e., $D_i = D_0/N_i$, where D_0 is the segmental diffusion coefficient and D_i is the effective diffusion coefficient of the center of mass of component i, with equal effective mobility of all monomers, the Onsager coefficient has a simple time-independent form

$$\Lambda = D_0 f(1-f) \tag{9}$$

and therefore

$$\frac{\partial}{\partial t}\psi(q) = -q^2 D_0 f(1-f)L(q,t)\psi(q) + \eta(q,t). \tag{10}$$

The solution of this linear differential equation is given by

$$\psi(t) = \int_0^t \exp\left\{-q^2 D_0 f(1-f)\int_\tau^t L(q,t')dt'\right\}\eta(q,\tau)d\tau. \tag{11}$$

For the kinetics of the chemical reactions taking place during the IPN formation there exists a finite time $t=t_c$ above which the separation kinetics of the IPN is suppressed, which is close to the gel time t_{gel}. Above this time the evolution of the separation kinetics is frozen and $\psi(t)$ becomes a static value $\psi_s=\psi(t)$, $t>t_c$. From this solution the structure factor $S(q)$ of the irreversible frozen fluctuations can be calculated as

$$S(q) = \langle\psi(q,t)^2\rangle = \int_0^{t_c}\int_0^{t_c}\exp\left\{-q^2 D_0 f(1-f)\int_\tau^{t_c}L(q,t')dt' - q^2 D_0 f(1-f)\int_{\tau'}^{t_c}L(q,t')dt'\right\}\langle\eta(q,\tau)\eta(q,\tau')\rangle d\tau d\tau'. \tag{12}$$

Because of equipartition the thermodynamic noise satisfies

$$\langle \eta(q,\tau)\,\eta(q,\tau')\rangle = \Delta_0 \delta(\tau-\tau'). \tag{13}$$

Thus the structure factor reduces to

$$S(q) = \Delta_0 \int_0^{t_c} \exp\left\{ -2q^2 D_0 f(1-f) \int_\tau^{t_c} L(q,t')dt' \right\} d\tau. \tag{14}$$

Use of the mean value law for the integration yields

$$S(q) = \Delta_0 \int_0^{t_c} \exp\{-2q^2 D_0 f(1-f) L(q)(t_c-\tau)\} d\tau, \tag{15}$$

with

$$L(q) = \left[\overline{A} q^2 + \overline{m} + \frac{\overline{C}}{q^2} \right], \tag{16}$$

in which $\overline{A}$, $\overline{m}$, and $\overline{C}$ are time-averaged effective values. The structure factor is then

$$S(q) = \frac{1-\exp[-\gamma L(q) q^2]}{q^2 L(q)} = \left[1 - \exp\left(-\gamma \frac{q^2}{S_0} \right) \right] \frac{S_0}{q^2}, \tag{17}$$

with

$$S_0 = \frac{1}{\overline{A} q^2 + \overline{m} + \dfrac{\overline{C}}{q^2}}; \tag{18}$$

in which γ is an effective coefficient which depends on the diffusion coefficient of the monomers, the composition ratio, and the kinetics of the IPN formation determined by t_c. It should be noted that as a result of using the mean value law for integration in the derivation of the structure factor $S(q)$, the values of the coefficients A, m, C, and γ differ from their actual values at time $t=t_c$, when the composition fluctuations are frozen. They represent effective mean values which depend on the thermodynamic history of the sample. Thus a simple physical interpretation of the coefficients is rather difficult. However, in contrast to the MST theories for homogeneous (ideal) IPN's the time-dependent structural evolution during network formation is taken into account, which seems to be necessary for real IPN's.[34]

It should be noted that S_0 has the same structure around the maximum given at $q=q^*$ as the structure factor S_{MST}, which reflects the fluctuations occurring in the disordered phase of a homogeneous IPN close to the microphase separation transition,[20]

$$S_{\mathrm{MST}}(x) = \frac{N_{\mathrm{eff}} f(1-f)}{\left[D(x/6) + \dfrac{x}{2+x} \right]^{-1} - 2\chi N_{\mathrm{eff}} f(1-f)}, \tag{19}$$

with $x = q^2 \langle R_{\mathrm{eff}}^2 \rangle$, R_{eff} the end-to-end distance between two mutual entanglements of the two subnetworks, and the Debye function $D(x) = 2x^{-2}[\exp(-x)+x-1]$. The length of the characteristic composition fluctuations of the ideal IPN is given by

$$l_{\mathrm{id}} = \frac{1}{q^*} \simeq \frac{\sqrt{\langle R_{\mathrm{eff}}^2 \rangle}}{2.33}. \tag{20}$$

In contrast to l_{id} the characteristic length determined by the coefficients of S_0,

$$l = \frac{1}{q^*} = \left(\frac{\overline{A}}{\overline{C}} \right)^{1/4}, \tag{21}$$

is an averaged length that represents the structural evolution during network formation, which is obtained by integrating from $t=0$ to $t=t_c$ in the derivation of $S(q)$ in Eq. (17). Due to this integration the structure factor, $S(q)$ given in Eq. (17) reveals a q^{-4} dependence at large q values. This result is in contrast to the structure factors which describe the fluctuations of polymer blends and block copolymers in the homogeneous phase close to a phase transition as well as for grafted networks, and ideal IPN's which all show a q^{-2} dependence at large q values. In the limit $q \to 0$ the structure factor vanishes for block copolymers, grafted networks, and ideal IPN's whereas $S(q)$ in Eq. (17) has a finite contribution.

B. Small-angle x-ray scattering

The relation between the absolute intensities from SAXS measurements $I(q)$ (e.u.^{2}/nm^3) and the derived structure factor $S(q)$ is given by

$$I(q) = V_z \Delta\eta^2 S(q), \tag{22}$$

with the scattering vector q defined as

$$q = \frac{4\pi}{\lambda} \sin\theta. \tag{23}$$

V_z denotes the volume per monomer unit of PCU, which can be estimated from the molecular weight M and the density ρ of the pure PCU network [ρ(PCU)=1.39 g/cm^3],

$$V_z = \frac{M}{\rho N_L}, \tag{24}$$

with $N_L = 6.02 \times 10^{23}$ mol^{-1}. $\Delta\eta$ is the electron density difference between the IPN phases which is determined from the experimental data by numerical integration using[32]

$$\Delta\eta^2 = \frac{1}{2\pi^2 f(1-f)} \int_{q_{\min}}^{q_{\max}} I(q) q^2 dq \tag{25}$$

($q_{\min}=0.12$ nm^{-1}, $q_{\max}=2.5$ nm^{-1}). Values for V_z and $\Delta\eta^2$ are given in Table I.

The scattering intensities $I(q)$ versus scattering vector q are shown in Fig. 2. For all samples $I(q)$ increases at small q values which indicates the existence of heterogeneous morphologies. For samples 1 and 2 (30 and 54 wt. % PCU) the increase in scattering intensity with decreasing q is much larger than for samples 3 and 4 with higher PCU content. The intensity for the pure PCU network is also given in Fig. 2, showing no characteristic scattering.

The log-log plots of intensity $I(q)$ versus q are shown in Fig. 3 . The scattering profiles of samples 1 and 2 (30 and 54 wt. % PCU) show a q^{-4} dependence for almost the entire

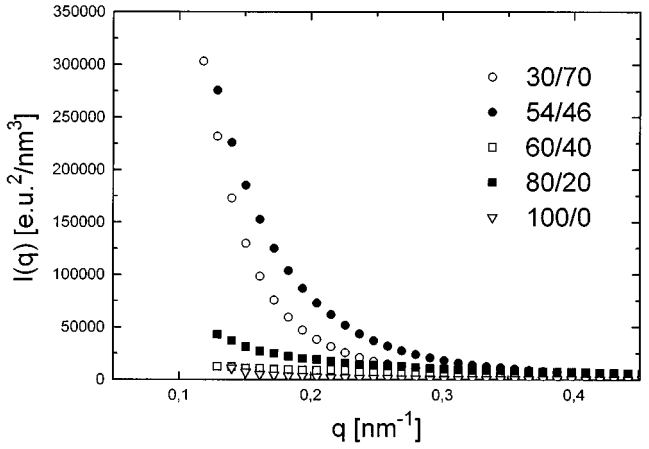

FIG. 2. Scattering intensity $I(q)$ versus scattering vector q of IPN's, and cross-linked PCU.

q range which corresponds to the well-known Porod law.[33] For sample 2 a slight deviation occurs at small q values. The scattering intensities for samples 3 and 4 (60 and 80 wt. % PCU) cannot be described by a q^{-x} dependence for the whole q range. At small q values x is smaller than 2 and it increases at large q values to about 6. The lines in Fig. 3 are fits by the structure factor $S(q)$ given by Eq. (17). The shapes of the scattering profiles and the theoretical structure factor are in good agreement. For samples 3 and 4 slight deviations occur at small and large q values.

Since $S_0(q)$ in Eq. (17) has a maximum at q^*, it is reasonable to plot the scattering data as $I(q)q^2$ versus q. The

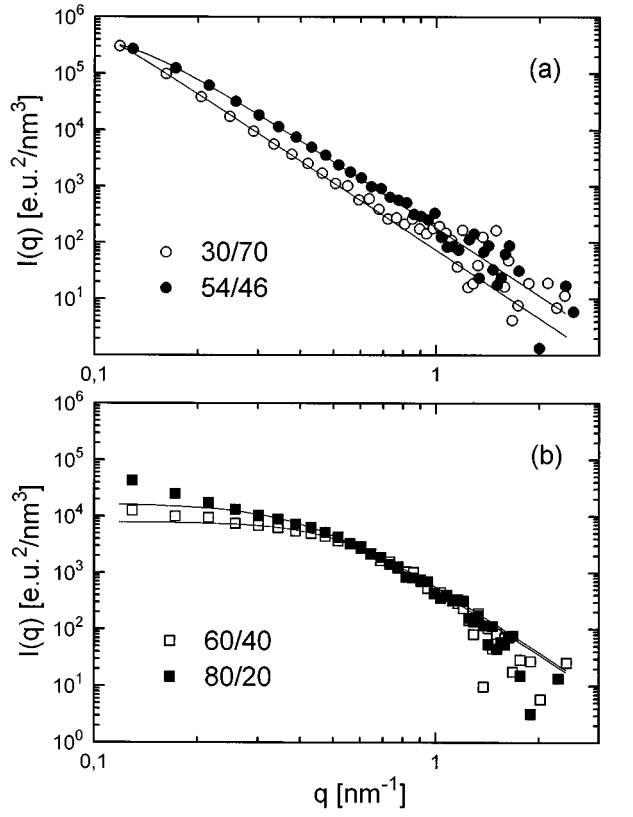

FIG. 3. Scattering intensity $I(q)$ versus scattering vector q of IPN's. The lines are fits by the structure factor $S(q)$ [Eq. (17)].

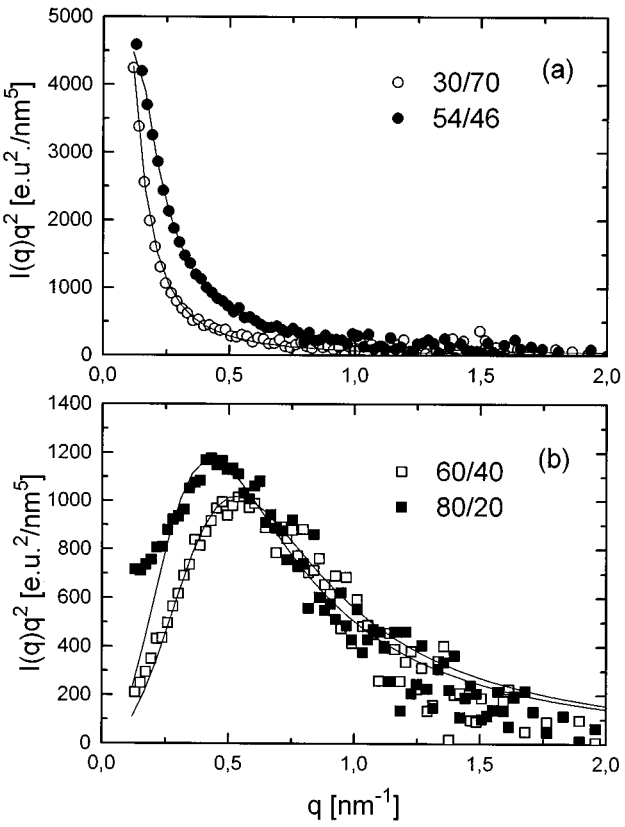

FIG. 4. Scattering intensity $I(q)q^2$ versus scattering vector q of IPN's. The lines are fits by the structure factor $S(q)$ [Eq. (17)].

profiles in Fig. 4 of IPN's with 60 and 80 wt. % PCU show the expected maximum in scattering intensity, whereas those of samples with 30 and 54 wt. % PCU increase continuously with decreasing q. The fits of the data using Eq. (17), which are identical to those in Fig. 3, are also plotted in Fig. 4. No pronounced maxima for samples 1 and 2 may indicate that q^* is below the resolution of the Kratky camera ($q_{\min} = 0.12\ \mathrm{nm}^{-1}$). The coefficients ($A$, m, C, and γ) and the characteristic length l [Eq. (21)] given in Table II were determined. The lengths are 1.9 and 2.3 nm for samples with 60 and 80 wt. % PCU and 33.2 and 15.2 nm for samples with 30 and 54 wt. % PCU. These values correspond to the averaged length of the frozen composition fluctuations that occur during IPN formation and which are frustrated due to increasing topological restraints by the growing network clusters. Samples 3 and 4 seem to have a finer morphology than samples 1 and 2. This result is in accordance with the DSC measurements and the transmission electron microscopy in Ref. 24. For samples 3 and 4, having one T_g, no microphase separated structures can be resolved whereas for samples 1 and 2 two glass transitions are determined corresponding to distinguished microphases in those IPN's. The values of the coefficients of the structure factor $S(q)$ may give insight into the chemical and physical processes during the formation of simultaneous IPN's, leading to the frozen composition fluctuations (microphases) in these materials. Starting from the one-phase mixture of monomers, cross-linkers, initiators, and catalysts the chemical polymerization and cross-linking reactions lead to growing network fragments and at a definite degree of conversion the two network components start to

TABLE II. Coefficients of $S(q)$ [Eq. (17)], characteristic length l of frozen microphases of IPN's as determined from the coefficients of $S(q)$ [Eq. (21)], and correlation length ξ and $S(0)$ of the Debye-Bueche structure factor $S_{DB}(q)$ [Eq. (26)].

PCU [wt. %]	$\overline{A}$	$\overline{m}$	$\overline{C}$	γ	l [nm]	ξ [nm]	$S(0)$
30	1.59	0.35×10^{-2}	1.3×10^{-6}	8592	33.2	23.3	22.6×10^{6}
54	1.18	2.27×10^{-2}	22.0×10^{-6}	3027	15.2	9.1	1.5×10^{6}
60	0.22	1.39×10^{-2}	1.8×10^{-2}	2722	1.9	1.8	0.12×10^{6}
80	0.45	5.89×10^{-2}	1.5×10^{-2}	398	2.3	2.2	0.21×10^{6}

phase separate due to thermodynamic immiscibility. This decomposition process is restricted by topological connections of network fragments, which lead to local attractive interactions represented by C. This coefficient is 10^4 times smaller for samples 1 and 2 than for samples 3 and 4. This large difference in the C values seems to herald the appearance of the second T_g. The coefficient γ which represents the relative mobility of the components during the network formation is larger for samples 1 and 2. So the restriction of the decomposition in these samples seems to be weaker as compared to samples 3 and 4, leading to a larger characteristic length l of the composition fluctuations. Finally the fluctuations are frustrated at time $t=t_c$ by the increasing irreversible topological restraints due to network growth. These results are in accordance with a recent Monte Carlo study of interpenetrating network formation[34] for a class of simultaneous IPN's including the system investigated in this paper.

In previous scattering experiments on IPN's the scattering data were analyzed by a statistical approach using the structure factor of Debye-Bueche,[35–37]

$$S_{DB}(q)=\frac{S(0)}{(1+\xi^2q^2)^2}, \tag{26}$$

which assumes a random distribution of phases with different sizes and shapes. A correlation function $\gamma(r)$ is used to describe structural features. For a multiphase system it gives the probability that two points separated by a distance r will still be in the same phase. In the Debye-Bueche approach an exponential correlation function is used,

$$\gamma(r)=\gamma(0)\exp(-\xi/r), \tag{27}$$

with the correlation length ξ. We also applied the Debye-Bueche law [Eq. (26)] to fit the scattering data. The quality of the fits is comparable to those using Eq. (17).

Values of $S(0)$ and ξ are given in Table II. The correlation lengths are 1.7 and 2.4 nm for samples with 60 and 80 wt. % PCU which are close to the averaged characteristic length determined by Eq. (21). The correlation lengths are 23.3 and 9.1 nm for samples with 30 and 54 wt. % PCU, respectively, which are at least of the order of magnitude of the corresponding characteristic length l.

The comparison of the structure factor in the hydrodynamic limit for IPN's and the Debye-Bueche theory which is used to describe the structure of different kinds of materials (glasses, foams, etc.) shows that they are in remarkable agreement. It is not trivial that l and ξ are equal or close since ξ in the Debye-Bueche theory is the correlation length of a final structure whereas l represents a time average of the characteristic length during the structural evolution of the IPN formation (see below). Therefore one can conclude that either the correlation length of fluctuations close to the pinning at time $t=t_c$ is represented with a large weight in the integration or that the structure having the final correlation length has been already developed at the very early stages of IPN formation. Although both approaches are in agreement with the scattering data, the structure factor derived in this paper is more appropriate for simultaneous IPN's since it takes the time-dependent evolution of the structure into account. In the special case of IPN formation consideration of the decomposition kinetics gives an adequate description of the experimental results in contrast to the MST theories for homogeneous (ideal) IPN's.

IV. CONCLUSION

The structure factor for IPN's derived in this work takes into account the frustration of the composition fluctuations by increasing topological restraints during network formation. In contrast to the structure factor $S_{MST}(q)$ for ideal IPN's the structure factor shows a finite contribution in the limit $q\to0$ and a q^{-4} dependence at large q values which corresponds to the well-known Porod behavior. The shape is comparable to the approach by Debye and Bueche $S_{DB}(q)$, which gives a very general description of the final structure by assuming a random distribution of sizes and shapes, but does not consider structural evolution of the microphases during IPN formation. The derived structure factor is in good agreement with the experimental small-angle x-ray scattering data for simultaneously cross-linked IPN's with a very fine morphology with a characteristic length of about 2 nm as well as for IPN's with larger microphases with a characteristic length between 10 and 35 nm.

ACKNOWLEDGMENTS

This work has been supported by the Bundesminister für Wirtschaft through the Arbeitsgemeinschaft Industrieller Forschungsvereinigungen e.V., Grant No. 9510, the German Academic Exchange Service (DAAD), the Deutsche Forschungsgemeinschaft, Grant No. schu 934/1-2, the National Science Foundation, Grant No. DMR-9023541, and the Donors of the Petroleum Fund of the American Chemical Society. The authors would like to thank Dr. P. Zhou for the preparation of the samples.

[1] J.W. Cahn and J.E. Hilliard, J. Chem. Phys. **28**, 258 (1958).
[2] P.G. de Gennes, J. Chem. Phys. **72**, 4757 (1980).
[3] K. Binder, J. Chem. Phys. **79**, 6387 (1983).
[4] T. Hashimoto, J. Kumaki, and H. Kawai, Macromolecules **16**, 757 (1983).
[5] H.C. Snyder and P. Meakin, J. Polym. Sci. Polym. Symp. **73**, 217 (1985).
[6] H. Meier and G. Strobl, Macromolecules **20**, 649 (1987).
[7] F.S. Bates and G.H. Fredrickson, Annu. Rev. Phys. Chem. **41**, 525 (1990).
[8] I. Alig, F. Kremer, G. Fytas, and J. Roovers, Macromolecules **25**, 5277 (1992).
[9] L. Leibler, Macromolecules **13**, 1602 (1980).
[10] P.-G. de Gennes, J. Phys. (Paris) Lett. **40,** L-69 (1979).
[11] R.M. Briber and B.J. Bauer, Macromolecules **21**, 3296 (1988).
[12] L.H. Sperling, *Interpenetrating Polymer Networks and Related Materials* (Plenum, New York, 1981).
[13] H.L. Frisch, Br. Polym. J. **17**, 149 (1985).
[14] Y.S. Lipatov, in *Advances in Interpenetrating Networks,* edited by D. Klempner and K.C. Frisch (Technomic, Lancaster, 1989), Vol. I.
[15] J.T. Koberstein and R.S. Stein, Polym. Eng. Sci. **24**, 293 (1984).
[16] B. McGarey, in *Advances in Interpenetrating Networks,* edited by D. Klempner and K.C. Frisch (Technomic, Lancaster, 1989), Vol. I.
[17] A. Brulet, M. Daoud, P. Zhou, and H.L. Frisch, J. Phys. (France) II **3**, 1161 (1993).
[18] D.S. Lee and S.C. Kim, Macromolecules **17**, 2193 (1984), and references therein.
[19] K. Binder and H.L. Frisch, J. Chem. Phys. **81**, 2126 (1984).
[20] M. Schulz, J. Chem. Phys. **97**, 5631 (1992).
[21] M. Schulz and K. Binder, J. Chem. Phys. **98**, 65 (1993); H.L. Frisch and A.Y. Grosberg, Makromol. Chem. (Theory Simulation) **2**, 517 (1993).
[22] R. Petschek and H. Metiu, J. Chem. Phys. **79**, 3443 (1983).
[23] J.H. An and L.H. Sperling, in *Cross-linked Polymers: Chemistry, Properties and Applications,* ACS Symposium Series No. 367, edited by R.A. Dickie, S.S. Labana, and R.S. Bauer (American Chemical Society, Washington, D.C., 1988).
[24] H.L. Frisch, P. Zhou, K.C. Frisch, X.H. Xiao, M.W. Huang, and H. Ghiradella, J. Polym. Sci. A **29**, 1031 (1991).
[25] P. Zhou and H.L. Frisch, J. Polym. Sci. A **31**, 3479 (1993).
[26] G. Strobl, Acta Crystallogr. A **26**, 367 (1970).
[27] P.G. de Gennes, *Scaling Concepts in Polymer Physics* (Cornell University Press, Ithaca, NY, 1979).
[28] P.J. Flory, *Principles of Polymer Chemistry* (Cornell University Press, Ithaca, NY, 1953).
[29] A. Bettachy, A. Derouiche, M. Benhamou, and M. Daoud, J. Phys. **1**, 153 (1991).
[30] S. Stepanow and M. Schulz, J. Chem. Phys. **98**, 6558 (1993).
[31] M. Doi and S.F. Edwards, *Theory of Polymer Dynamics* (Wiley, New York, 1987).
[32] F.J. Baltá-Calleja and C.G. Vonk, in *X-Ray Scattering of Synthetic Polymers,* edited by A.D. Jenkins (Elsevier, New York, 1989).
[33] G. Porod, Kolloid Z. **124**, 83 (1951); **125**, 51 (1952); **125**, 108 (1952).
[34] M. Schulz and H.L. Frisch, J. Chem. Phys. **101**, 10 008 (1994).
[35] P. Debye and A.M. Bueche, J. Appl. Phys. **20**, 518 (1949).
[36] P. Debye, H. Anderson, and H. Brumberger, J. Appl. Phys. **28**, 679 (1957).
[37] J. Lal, J.M. Widmaier, J. Bastide, and F. Boue, Macromolecules **27**, 6443 (1994).